IS 77-138
PREPRINT UCRL- 79521

CONF-770661--1

Lawrence Livermore Laboratory

RYDBERG SERIES IN THE LANTHANIDES AND ACTINIDES OBSERVED BY STEPWISE LASER EXCITATION

E.F. Worden, R.W. Solarz, J.A. Paisner, K. Rajnak, B.W. Shore, and J.G. Conway

May 18, 1977

This Paper was Prepared For Submission To:

International Conference on Atomic and Molecular States Coupled to a Continuum-Highly Excited Atoms and Molecules, June 13-17, 1977, Aussois, France.

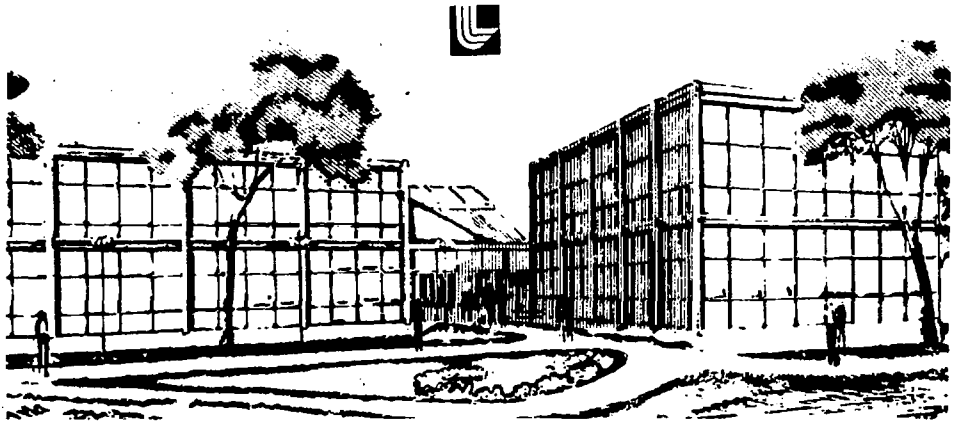

RYDBERG SERIES IN THE LANTHANIDES AND ACTINIDES OBSERVED BY STEPWISE LASER EXCITATION*

E.F. Worden, R.W. Solarz, J.A. Paisner, K. Rajnak, B.W. Shore
Lawrence Livermore Laboratory
Livermore, California 94550

J.G. Conway
Lawrence Berkeley Laboratory
Berkeley, California 94720

Prepared for Submission to the International Conference on Atomic and Molecular States Coupled to a Continuum-Highly Excited Atoms and Molecules, June 13-17, 1977, Aussois, France.

ABSTRACT:

The techniques of stepwise laser excitation have been applied to obtain Rydberg series in the lanthanides and in uranium. The methods employed circumvent many of the experimental difficulties inherent in conventional absorption spectroscopy of these heavy atoms with very complex spectra. The Rydberg series observed have allowed the determination of accurate ionization limits. The values in eV are: Ce, 5.5387(4); Nd. 5.5250(6); Sm, 5.6437(10); Eu, 5.6704(3); Gd, 6.1502(6); Tb, 5.8639(6); Dy, 5.9390(6); Ho, 6.0216(6); Er 6.1077(6); U, 6.1941(5). A comparison of the $f^n s^2$ - $f^n s$ ionization limits as a function of n with theoretical calculations is made.

* Work performed under the auspices of the U.S. Energy Research & Development Administration under contract No. W-7405-Eng-48.

RYDBERG SERIES IN THE LANTHANIDES AND ACTINIDES OBSERVED BY STEPWISE LASER EXCITATION

E.F. Worden, R.W. Solarz, J.A. Paisner, K. Rajnak, B.W. Shore
Lawrence Livermore Laboratory, Livermore, California 94550

J.G. Conway
Lawrence Berkeley Laboratory, Berkeley, California 94720

The observation of Rydberg series in most of the lanthanides and in the actinides by conventional absorption spectroscopy is extremely difficult if not impossible. This is caused by the extreme complexity of the electronic structure of most of the lanthanide and actinide elements. The spectra of these heavy atoms are very complex and characterized by weak absorptions, especially into Rydberg states with large principal quantum numbers. The presence of a number of populated low lying levels in most of the atoms of these elements together with the great density of potentially perturbing valence levels at high energy so complicates most of the single photon absorption spectra that Rydberg series cannot be sorted out. Indeed, the only elements of these two groups where Rydberg series have been observed by conventional spectroscopy have relatively simple spectra and very few low lying energy levels.[1-4] The elements lanthanum,[1] europium,[2] thulium,[3] ytterbium[4] and lutetium[4] all have only one or two well isolated low levels that are thermally populated at the temperatures needed to produce an atomic vapor and have only a few well separated ion levels to serve as Rydberg convergence limits. For the remaining elements with complex spectra more sensitive and flexible methods are required for the observation of well developed Rydberg series.

Recently stepwise laser photoexcitation and ionization has been used in our Laboratory to identify Rydberg series in uranium[5]. The methods offer a number of advantages over conventional photoabsorption techniques. They allow access to a variety of states with the ability to populate a single specific level. This avoids the difficulty of sorting out which of the thermally populated levels is associated with a specific absorption feature. The methods are sensitive and when required, time resolution can be employed. The delayed ionization step allows greater assurance that a Rydberg series can be obtained. The methods we use are similar to those used by Stebbings and Dunning[6] for bound level and autoionization studies. We have applied the multistep photoionization methods to obtain Rydberg series in ten lanthanides and uranium. This has permitted us to obtain accurate ionization limits for these elements. We will show that the $f^n s^2$ to $f^n s$ ionization potentials when plotted against n for the lanthanides form two straight lines, one for each half of the f-shell. Theory predicts such a behavior for lowest level to lowest level ionization potential for the $f^n s^2$ - $f^n s$ configurations. A relatively simple physical explanation can be given.

In this paper we will describe the stepwise laser photoionization techniques and the experimental apparatus we have employed. Then we will show some of the Rydberg series obtained by these techniques and give a comparison of the ionization limits obtained by our techniques with those obtained by other methods. Finally we will discuss the relationship between the ionization potentials and number of f electrons in the lanthanides.

A schematic of the type of experimental apparatus used in our laboratories is shown in Figure 1. Descriptions have been published.[5,7] We have two such facilities and the actual set up varies according to the specific experiment. The apparatus is a crossed beam spectrometer in which the atoms in the atomic beam are irradiated and eventually ionized by the output of either two or three commerical nitrogen laser pumped tunable dye lasers. The oven consists of a resistively heated tungsten tube containing a tungsten crucible holding the metal to be vaporized. The oven is usually operated at a temperature sufficient to give a vapor pressure of approximately 10^{-3} Torr (0.1 Pascal) of the atomic species under study. The vapor issues into an interaction chamber that is electrically biased to suppress thermal and surface ions and to efficiently collect and direct photoion products into the detection system. The detector is a channeltron particle multiplier contained in a quadrupole mass analyzer. A mass resolution of one a.m.u. is normally used. The quadrupole is tuned to the mass of the atom under study and serves to discriminate against detection of oxide or other impurities. The vacuum chamber background pressure is typically 10^{-7} Torr (10^{-5} Pascal).

Other lasers such as a CO_2 laser can be added to the system or a high resolution pressure tuned dye laser can replace one of the commerical nitrogen laser pumped dye lasers. Furthermore, the interaction chamber can be replaced by a field ionization chamber and channeltron ion detector. Here caution is excercised to avoid oxide or other unwanted photoion signals because quadrupole selection is no longer used.

The nitrogen pump lasers are triggered by a common master control unit that initiates each laser at predetermined and well controlled times with respect

to one another (typically <3 ns). The desired delay between the firing of any of the lasers can be adjusted by inserting an appropriate length of cable or using a preprogrammed delay system of 0 to 600 ns. This assures obtaining the desired excitation sequence.

The first and/or second lasers are tuned to the specific wavelength(s) to populate the desired level(s). The final laser in the excitation sequence (either the second or third laser) is then scanned to obtain the Rydberg or autoionization spectrum. This spectrum and wavelength calibrations are recorded simultaneously on a two pen recorder. Wavelength calibration is obtained by directing a portion of the scan laser radiation to a 1.5 m Jobin-Yvon monochromator that is preset at known U or Th emission lines from an electrodeless lamp. The nitrogen pumped dye lasers typically have pulse widths of 5 ns and line widths of 0.2 to 0.5 $\mathring{A}$ (.5 to 2 cm^{-1}).

Some of the excitation schemes employed to obtain the Rydberg series are shown in Figure 2. The primary excitation (λ_1) is always a known transition from the ground or low lying thermally populated level. (In our notation λ_n is the wavelength of the nth laser in the excitation sequence.) In the three step experiments λ_2 is usually a known transition, but occasionally it is necessary to use a transition obtained by laser spectroscopy techniques where λ_1 is fixed, λ_2 is scanned and λ_3 is fixed at a wavelength such that the energy of $\lambda_2 + \lambda_2 + \lambda_3$ exceeds the ionization potential of the element. Ion current is obtained when λ_2 coincides with an allowed transition from the level populated by λ_1. The details of this method have been described previously.[7] Such searches were performed when sufficient levels in the 3-4 eV range of the correct parity were not known.

All excitation sequences are subject to background peaks. For two laser excitations and depending on the wavelengths of λ_1 and λ_2, $2\lambda_2$ peaks from the ground or thermally populated levels or $3\lambda_2$ peaks may be present. When using 3 lasers, $\lambda_1 + 2\lambda_3$ or $3\lambda_3$ peaks may occur. Background scans are performed blocking λ_1 and/or λ_2 and repeating the λ_2 or λ_3 scan to determine those peaks not due to $\lambda_1 + \lambda_2$ or to $\lambda_1 + \lambda_2 + \lambda_3$ in each case.

As indicated on the figure, several methods of ionization were employed to observe series. In most cases (Nd, Sm, Eu, Dy, Ho, and Er), autoionizing Rydberg series converging to an excited state of the ion were obtained. For lanthanides with very complex spectra (cerium, gadolinium and terbium), field ionization was used. The field was applied 2 to 5 microseconds after the populating laser λ_2 or λ_3. This time resolution allowed radiative decay of some of the shorter lived valence levels and facilitiated preferential detection of Rydberg levels that are longer lived. Collisional ionization was used to observe a series in holmium. In this case, the oven temperature was increased until the atom density was such that the bound Rydberg levels were ionized and a long series was obtained. Series in uranium were obtained by time resolved CO_2 laser ionization and by time resolved field ionization. These techniques have been described previously.[5]

In all cases except gadolinium and terbium, a rough ($\pm$ 40 cm^{-1}) determination of the ionization potential was obtained by the observation of the photoionization threshold. Gadolinium and terbium were determined last and predicted values were used to estimate the wavelength range to search for Rydberg series. The photoionization thresholds were observed using two and/or three step excitation techniques. Typical photoionization threshold scans are shown in Fig. 3. These are for Nd with the excitation sequences used being shown in the figure. The threshold is marked by the onset of very strong autoionizing levels. In

addition, a continuous absorption due to ionization is usually present. Scan (a) shows very few ionization peaks of the type $\lambda_1 + 2\lambda_2$ before the onset of $\lambda_1 + \lambda_2$ ionization so that the threshold is very easily recognized. In scan (b) a number of $\lambda_1 + 2\lambda_2$ peaks precede the threshold but the strength of the autoionizing peaks and continuous absorption make identification of the threshold easy. This is not always the case, and some identifications were more difficult.

The photoionization thresholds observed for the lanthanides by two step excitation methods are shown in Table 1 and those observed by three step excitation methods are shown in Table 2. The reproducibility of the values obtained from different parent levels and from the two schemes was better in some cases but all values agree to within $\pm$ 60 cm^{-1} or less.

From the photoionization threshold results, wavelength ranges to search for bound Rydberg series with field or collisional ionization or to search for autoionizing series converging to excited states of the ion were estimated for various parent levels that could be conveniently populated by one or two step excitations. Scans were made until series were obtained. Typical Rydberg spectra for europium, dysprosium, holmium and cerium are shown in Fig. 4 through 7.

The variation in quantum defect (n - n*) versus n with change in assumed limit value for cerium is shown in Fig. 8. The value of n is not necessarily the principal quantum number but is an integer chosen close to n* in order to evaluate variation in quantum defect. The equation for n* is shown on the figure. Our criterion for choosing the ionization limit of the element is to select the assumed limit that gives the smoothest and most constant value of the quantum defect as a function of n.

We realize that our series are subject to perturbation by members of other Rydberg series and by certain valence levels. These can cause substantial variations in the quantum defect from level to level. In cases when perturbations are evident our uncertainties have been adjusted accordingly. Much more accurate limits could be obtained from high resolution scans (.03 cm^{-1} vs ~1 cm^{-1}) and by applying multichannel quantum defect theory (MQDT) to analyze the perturbations. Application of the techniques by others to a number of atomic and molecular spectra recently has permitted extended assignments in perturbed Rydberg series and precise ionization limits ($\pm$ 0.1 cm^{-1} or better) to be obtained.[8] The application of MQDT to heavy atoms with complex spectra is very difficult because of the large number of possible channels. Table 3 shows the number of channels accessible from the J = 6, odd level in uranium at 32900.087 cm^{-1}. Even if limited to levels converging to the ground and first excited level of the ion and low angular momentum running electrons there are 20 channels anticipated. Preliminary analysis of the data indicates that many features of the spectrum can be recovered in a two limit analysis and that the ionization limit quoted earlier is in fact correct within the stated margin of error.

The ionization potentials obtained for the lanthanides from the observed Rydberg series are given in Table 4. The excitation wavelengths and levels from which the series were observed and the ion levels that they converge to are indicated in the table. Information on ionic states was obtained

from the National Bureau of Standards monograph 145 and references contained therein.[9] The values from different parent levels and different convergence limits give the same value within the estimated uncertainties in each case. This agreement substantiates the reliability of our method. In addition, our measured value of the limit in europium, 45734(2) cm^{-1}, is in excellent agreement with the absorption study of Tomkins and Smith[2] who obtained 45734.9(2) cm^{-1}.

A summary of the ionization limits obtained by various methods for the lanthanides is shown in Table 5. The less accurate electron impact values[10] agree with our results within their estimated uncertainties except for erbium. Surface ionization results,[11] not shown here, are low when compared with Camus' accurate values for thulium and ytterbium.[4] The spectroscopic extrapolation values of Reader and Sugar[12] are in better agreement but the cerium, praseodymium, and neodymium values are low.

With the exception of Ce and Gd, the ionization process is the removal of an s electron for the $4f^N6s^2$ (N = 2 to 14) configuration. That is the ionization potential is the difference between the energy of the lowest level of the $4f^N6s^2$ configuration of the neutral and the lowest level of the $4f^N6s$ configuration of the ion. For Ce (N = 2) and Gd (N = 8) the lowest lying configuration for the neutral and ion are $f^{N-1}ds^2$ and $f^{N-1}d^2$ and $f^{N-1}ds^2$ and $f^{N-1}ds$, respectively. However, the position of the lowest lying levels of the f^Ns^2 and f^Ns configuration are known very accurately from spectroscopic studies. We can therefor normalize our results so that all ionization limits correspond to the removal of an s electron from the lowest lying level of the f^Ns^2 configuration. The resulting data is plotted in Fig. 9. The values for Tm and Yb are taken

from Camus. The ionization limits normalized in this way clearly show a piecewise linear variation with a change of slope at the half-filled shell (N = 7). This behavior is not unusual as illustrated in Figs. 10 and 11 in which the normalized ionization limits for the first short period ($2p^N2s^2 - 2p^N2s$) and the iron transition series ($3d^N4s^2 - 3d^N4s$) are plotted as a function of N. In all cases the limit corresponding to the difference in the lowest levels of the $\ell^N s^2$ configuration of the neutral and $\ell^N s$ of the ion has the same characteristic linear dependence on N with a slope break at the half-filled shell. An explanation of this behavior follows.

The Pauli principle, expressed as the requirement of particle-exchange antisymmetry of the combined space-spin wavefunction, forces a correlation between spin and spatial symmetry. In turn the enforced many-electron spatial symmetry affects the interelectron Coulomb repulsion: the repulsion is least, and hence the binding is greatest, when the spatial wavefunction is completely antisymmetric -- as occurs when all spins are aligned. This spin-enforced symmetry energy, a correlation energy, is responsible for splitting of spectroscopic terms; it is the mechanism underlying Hund's rule that the term of highest multiplicity has lowest energy. This energy obviously increases in magnitude in proportion to the number of aligned spins. Thus it increases as an election shell is filling. Once the shell becomes half-filled, further

electrons must pair their spins; hence the effect subsequently diminishes. Paired s-electrons make no contribution to this symmetry-dependent energy; only the ion, with it's single s electron is affected by the spin alignment of the partially filled shell.

An exact theoretical treatment of ionization energies lies beyond current capability. However, numerous approximate theories provide useful insight.

The simplest of these is the Slater-Condon semiempirical method, wherein we express expectation values of the Hamiltonian in terms of single-particle integrals and two-particle Coulomb-repulsion Slater integrals. Elementary application of this theory suggest that the ionization energy I_N of the configuration $\ell^N s^2$ (to yield $\ell^N s$) should follow the pattern

$$I_N = A + NB \qquad N \leq 2\ell + 1$$
$$= A + N[B + G_\ell(\ell,s)], \quad N > 2\ell + 1 .$$

That is, the ionization energy as a function of N follows a straight-line curve broken at the half-filled shell value $N = 2\ell + 1$. The change in slope is simply the exchange integral $G_\ell(\ell,s)$ of the ion. A and B are simply combinations of other Slater parameters.

A more elaborate approach is to employ ab-initio Hartree-Fock theory to calculate the ionization energies. Computations at LLL based on this approach give this same broken straight-line behavior.

A least-squares fit to our experimental data yields a slope difference of 220 ($\pm$ 21.5) cm^{-1}. This value is in excellent agreement with the approximate average experimental value of $G_3(f,s)$, 207 cm^{-1}, for the lanthanides.[13] It is

also in good agreement with the slope difference obtained in Hartree-Fock computations. This agreement supports the interpretation of the broken-line curve as originating with the exchange effect.

In view of this trend, an attempt is in progress to extend the method to extrapolate the ionization potentials of the heavy actinides. This appears worthwhile since experimental values are not likely to be obtained in the near future.

In conclusion, a variety of laser spectroscopic methods have been used to identify Rydberg series and to monitor autoionization spectra in complex atomic systems. We have demonstrated that by using stepwise selective excitation and time resolved techniques together with the sensitivity of photoionization spectroscopy, one can study Rydberg levels of even the most complicated atomic species. The ionization limits we have obtained are 10 to 100 times more precise than values available previously. The precise values led to the discovery of the piece-wise linear behavior of $\ell^n s^2 - \ell^n s$ ionization potentials across the various series of the periodic table. Using high resolution lasers, it also appears that MQDT can be profitably applied to the analysis of the resulting spectra. It is clear that greatly extended analyses of highly excited states in the heavy atoms are now possible.

Figures

Tables

References

1. W. R. S. Garton and M. Wilson, Astrophys. J. 145, 333(1966).

2. G. Smith and F. S. Tomkins, Proc. Roy. Soc. Lond. A342, 149(1975). Phil. Trans. Roy. Soc. Lond. 283, 345(1976).

3. P. Camus and F. S. Tomkins, J. Physique 30, 545(1969).

4. P. Camus, Thesis, University of Paris, Orsay 1971.

5. R. W. Solarz, C. A. May, L. R. Carlson, E. F. Worden, S. A. Johnson, J. A. Paisner, and L. J. Radziemski, Phys. Rev. A 14, 1129-1136 (1976).

6. F. B. Dunning and R. F. Stebbings, Phys. Rev. A9, 2378(1974) and R.D. Rundel, F. B. Dunning, H. C. Goldwire, Jr., and R. F. Stebbings, J. Opt. Soc. Am. 65, 628 (1975).

7. L. R. Carlson, J. A. Paisner, E. F. Worden, S. A. Johnson, C. A. May, and R. W. Solarz, J. Opt. Soc. Am. 66, 846-853 (1976).

8. P. Esherick, J. A. Armstrong, R. W. Dreyfus, and J. J. Wynne, Phys. Rev. Lett. 36, 1296 (1976) and K. T. Lu and U. Fano, Phys. Rev. A2, 81 (1970).

9. W. F. Meggers, C. H. Corliss and B. F. Scribner, "Tables of Spectral-Line Intensities Part I - Arranged by Elements" N.B.S. monograph 145 (U.S. Government Printing Office, Washington, 1975).

10. R. J. Ackermann, E. G. Rauh and R. J. Thorn, J. Chem Phys. 65, 1027 (1976).

11. G. R. Hertel, J. Chem. Phys. 48, 2053 (1968).

12. J. Reader and J. Sugar, J. Opt. Soc. Am. 56, 1189 (1966).

13. B. G. Wybourne, "Spectroscopic Properties of the Rare Earths" (Wiley & Sons, New York 1965) p. 56, and J. Sugar and J. Reader, J. Opt. Soc. Am. 55, 1286 (1965).

Table 1. Two step photoionization threshold results.[a]

Element	λ_1 (Å)	Excited Level Used (cm^{-1})	λ_2 (Å)	Ionization Threshold[b,c] (cm^{-1})	(eV)
Ce	4632.32	21581.41	4338.2	44626(50)	5.533(6)
	4610.46	21683.74	4351.7	44657(50)	5.537(6)
	4583.10	21813.23	4370.7	44686(50)	5.540(6)
Pr	4939.74	23085.08	4764	44070(40)	5.464(5)
	3945.41	26715.34	5762	44065(40)	5.463(5)
Nd	4634.24	21572.61	4352.2	44543(20)	5.523(3)
	4924.53	20300.84	4124.1	44542(20)	5.522(3)
	4954.78	20176.90	4103.4	44543(20)	5.523(3)
	5056.89	19769.49	4352.2	44543(20)	5.523(3)
Sm	4226.18	24467.27	4756.7	45484(20)	5.639(3)
	4596.74	22041.02	4263.2	45491(20)	5.640(3)
Eu	4594.03	21761.26	4181.0	45672(20)	5.663(3)
	4661.88	21444.58	4118.2	45720(20)	5.669(3)
Dy	4565.09	21899.22	3847.5	47882(20)	5.937(3)
	4589.35	21783.42	3831.1	47879(20)	5.936(3)
	4612.26	21675.28	3822.2	47831(20)	5.931(3)
Ho	4040.81	24740.52	4206.0	48509(20)	6.014(3)
	4053.93	24660.46	4185.5	48546(20)	6.019(3)
Er	4087.63	24457.15	4034.2	49238(20)	6.105(3)

[a] Excitation wavelengths (λ_1) and excited level values are from NBS monograph 145 (Ref. 10) and references therein.

[b] Error limits are generally larger than the precision of the threshold determination because of the discrepancy between these values and the Rydberg convergence values.

[c] 8065.479 cm^{-1}/eV was used to convert the values from cm^{-1} to eV.

Table 2. Three step photoionization threshold results.[a]

Element	λ_1 (Å)	λ_2 (Å)	Excited Level Used (cm^{-1})	λ_3 (Å)	Ionization Threshold[b,c] (cm^{-1})	(eV)
Ce	6310.10	6996.8	30131(2)	6883.0	44656(20)	5.539(3)
Eu	6291.34	6787.48	30619.49	6621.2	45718(20)	5.668(3)
Dy	6259.09	6769.79	30739.79	5831.1	47884(20)	5.937(3)
Ho	6305.36	6576.8	31056(2)	5720.0	48534(20)	6.017(3)
	6305.36	6901.1	30342(2)	5495.0	48535(20)	6.018(3)
	6305.36	6947.1	30246(2)	5462.1	48549(20)	6.019(3)
Er	6221.02	6388.19	31719.65	5706.8	49238(20)	6.105(3)
	6221.02	6451.56	31565.94	5655.6	49243(20)	6.105(3)
	6221.02	6649.06	31105.66	5516.1	49230(20)	6.104(3)

[a]Excitation wavelengths (λ_1 and λ_2) and excited level values are from NBS monograph 145 (Ref. 10) and references therein except for Ce and Ho which were determined by laser techniques.

[b]Error limits are generally larger than the precision of the threshold determination because of the discrepancy between these values and the Rydberg convergence values.

[c]8065.479 cm^{-1}/eV was used to convert the cm^{-1} values to eV.

Table 3.

POSSIBLE BOUND RYDBERG CHANNELS IN URANIUM FROM A J = 6 LEVEL.

$I_m(cm^{-1})$	$[\beta J_c]^\circ$	$\varepsilon_m \ell j$	J
$I_1 = (49958.1)^a$	$5f^3 7s^2[{}^4I_{9/2}]^\circ$	$\varepsilon_1 p1/2$	5
$I_1 = (49958.1)^a$	$5f^3 7s^2[{}^4I_{9/2}]^\circ$	$\varepsilon_1 p3/2$	5,6
$I_1 = (49958.1)^a$	$5f^3 7s^2[{}^4I_{9/2}]^\circ$	$\varepsilon_1 f5/2$	5,6,7
$I_1 = (49958.1)^a$	$5f^3 7s^2[{}^4I_{9/2}]^\circ$	$\varepsilon_1 f7/2$	5,6,7
$I_2 = I_1 + 289.04$	$5f^3 6d7s[{}^6L_{11/2}]^\circ$	$\varepsilon_2 p1/2$	5,6
$I_2 = I_1 + 289.04$	$5f^3 6d7s[{}^6L_{11/2}]^\circ$	$\varepsilon_2 p3/2$	5,6,7
$I_2 = I_1 + 289.04$	$5f^3 6d7s[{}^6L_{11/2}]^\circ$	$\varepsilon_2 f5/2$	5,6,7
$I_2 = I_1 + 289.04$	$5f^3 6d7s[{}^6L_{11/2}]^\circ$	$\varepsilon_2 f7/2$	5,6,7

[a]reference 5

Table 4. Some lanthanide Rydberg series limits.

Element	λ_1[a] (Å)	λ_2[a,b] (Å)	Excited Level Used (cm^{-1})	Convergence Energy (cm^{-1})	Convergence Level in Ion (cm^{-1})	First Ionization Limit[c] (cm^{-1})	(eV)
Ce	3793.83		26331.11	44674(3)	0.00	44674(3)	5.5389(4)
	3873.03		27091.56	44671(3)	0.00	44671(3)	5.5385(4)
Nd	4924.53		20300.84	45075(5)	513.32	44562(5)	5.5250(6)
Sm	4596.74		22041.02	45846(8)	326.64	45519(8)	5.6437(10)
Eu	4594.03		21761.26	47403(2)	1669.21	45734(2)	5.6703(3)
	4661.88		21444.58	47405(2)	1669.21	45736(2)	5.6706(3)
	6291.34	6787.48	30619.49	47403(2)	1669.21	45734(2)	5.6703(3)
Gd	5617.91	6351.72	33534.71	49603(5)	0.00	49603(5)	6.1501(6)
	5701.35	6573.83	32957.77	47604(5)	0.00	49604(5)	6.1502(6)
Tb	4139.06		24438.76	47295(5)	0.00	47295	5.8639(6)
	4146.96		24392.75	47294(5)	0.00	47294	5.8638(6)
Dy	4211.72		23736.60	48730(5)	828.31	47902(5)	5.9391(6)
	6259.09	6769.79	30739.79	48727(5)	828.31	47899(5)	5.9388(6)
Ho	4103.04		24360.55	49203(5)	637.4	48566(5)	6.0216(6)
	6305.36	6947.1	30246(2)	48567(5)	0.00	48567(5)	6.0216(6)
Er	4087.63		24457.15	49704(5)	440.43	49264(5)	6.1080(6)
	6221.02	6451.56	31565.94	49699(5)	440.43	49259(5)	6.1074(6)

[a]Excitation wavelengths (λ_1 and λ_2) and excited level values given to 0.01 are from NBS monograph 145 and Refs. therein (Ref. 10).

[b]No value of λ_2 is given for two step observations when λ_2 is scanned. Values given are λ_2 for three step results.

[c]8065.479 cm^{-1}/eV used to convert values for cm^{-1} to eV.

Table 5. Comparison of Lanthanide First Ionization Potentials

Element	Electron[a] Impact	Spectroscopic[b] Extrapolation	Laser Spectroscopy LLL Photoionization Threshold	Laser Spectroscopy LLL Rydberg Convergence
Ce	5.44(10)	5.47(5)	5.537(4)	5.5387(4)
Pr	5.37(10)	5.42(3)	5.464(6)	---
Nd	5.49(10)	5.489(20)	5.523(3)	5.5250(6)
Pm	---	5.554(20)	---	[5.582(10)]
Sm	5.58(10)	5.631(20)	5.639(3)	5.6437(10)
Eu	5.68(10)	5.666(7)	5.666(3)	5.6704(3)
Gd	6.24(10)	6.141(20)	---	6.1502(6)
Tb	5.84(10)	5.852(20)	---	5.8639(6)
Dy	5.90(10)	5.927(8)	5.936(3)	5.9390(6)
Ho	5.99(10)	6.018(20)	6.017(3)	6.0216(6)
Er	5.93(10)	6.101(20)	6.104(3)	6.1077(6)
Tm	6.11(10)	6.18(2)	---	6.1844(2)[c]
Yb	6.21(10)	6.25(2)	---	6.2540(2)[c]

( ) = error in last digit

[ ] = extrapolated value

[a] R.J. Ackermann, E.G. Rauh and R.J. Thorn, J. Chem. Phys. 65, 1027 (1976).

[b] J. Reader and J. Sugar, J. Opt. Soc. Am. 56, 1189 (1966); update, W.C. Martin, L. Hagan, J. Reader and J. Sugar, Phys. Chem. Ref. Data 3, 771 (1974).

[c] P. Camus, Thesis, University of Paris, Orsay, 1971.

Laser spectroscopy apparatus

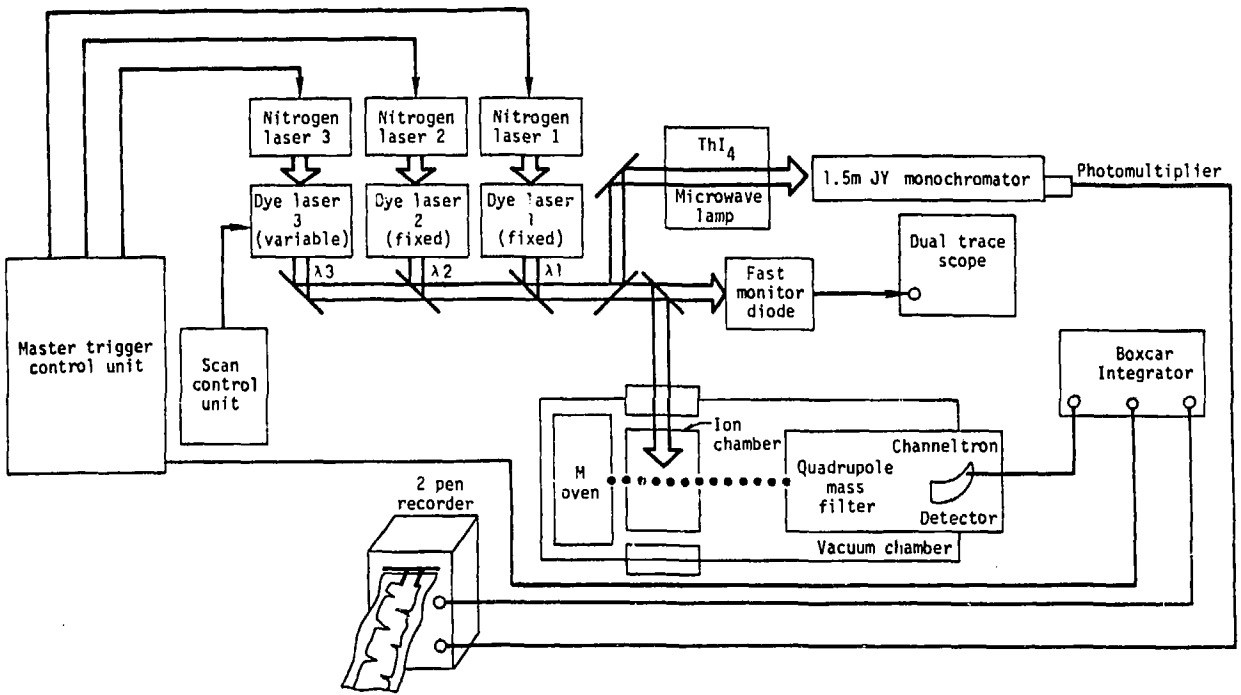

M = lanthanide or other metal

Figure 1

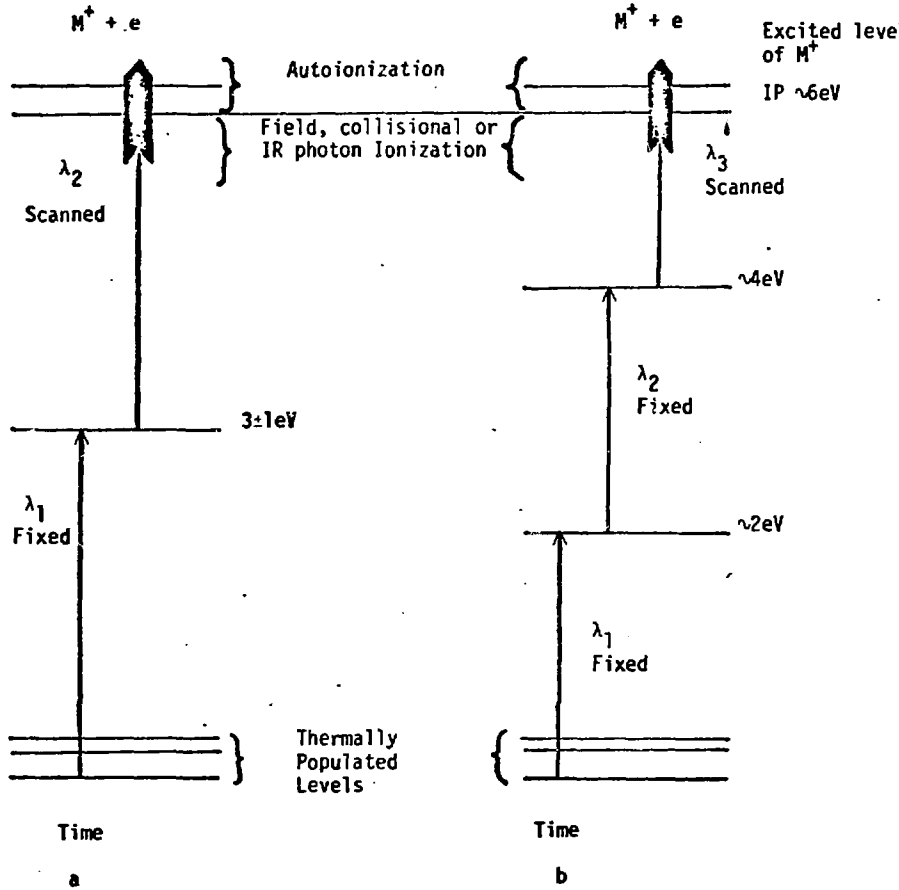

Figure 2. Excitation schemes used to obtain Rydberg and autoionization spectra.

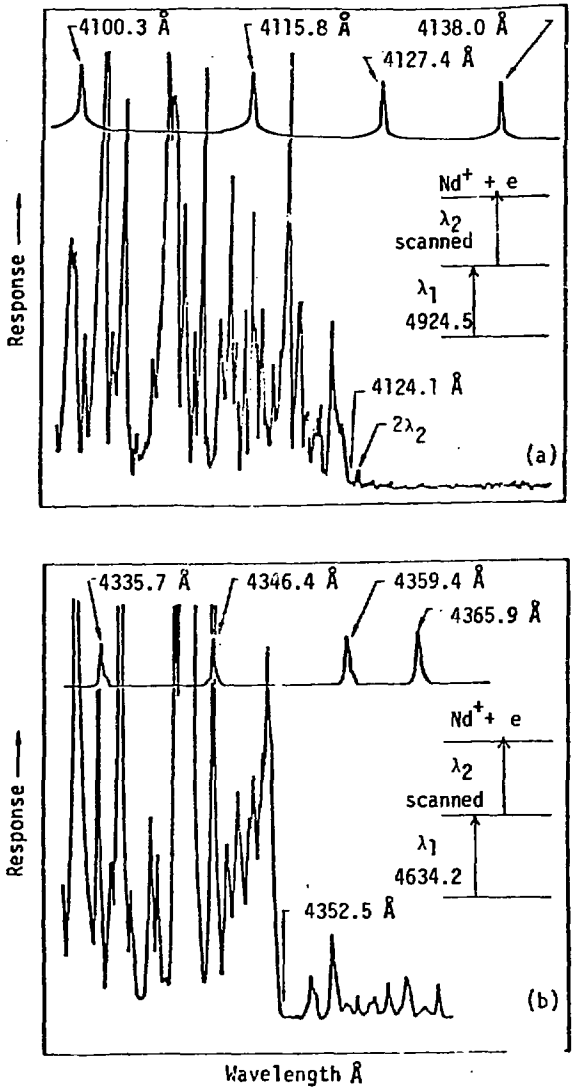

Figure 3. Photoionization Threshold in Neodynium

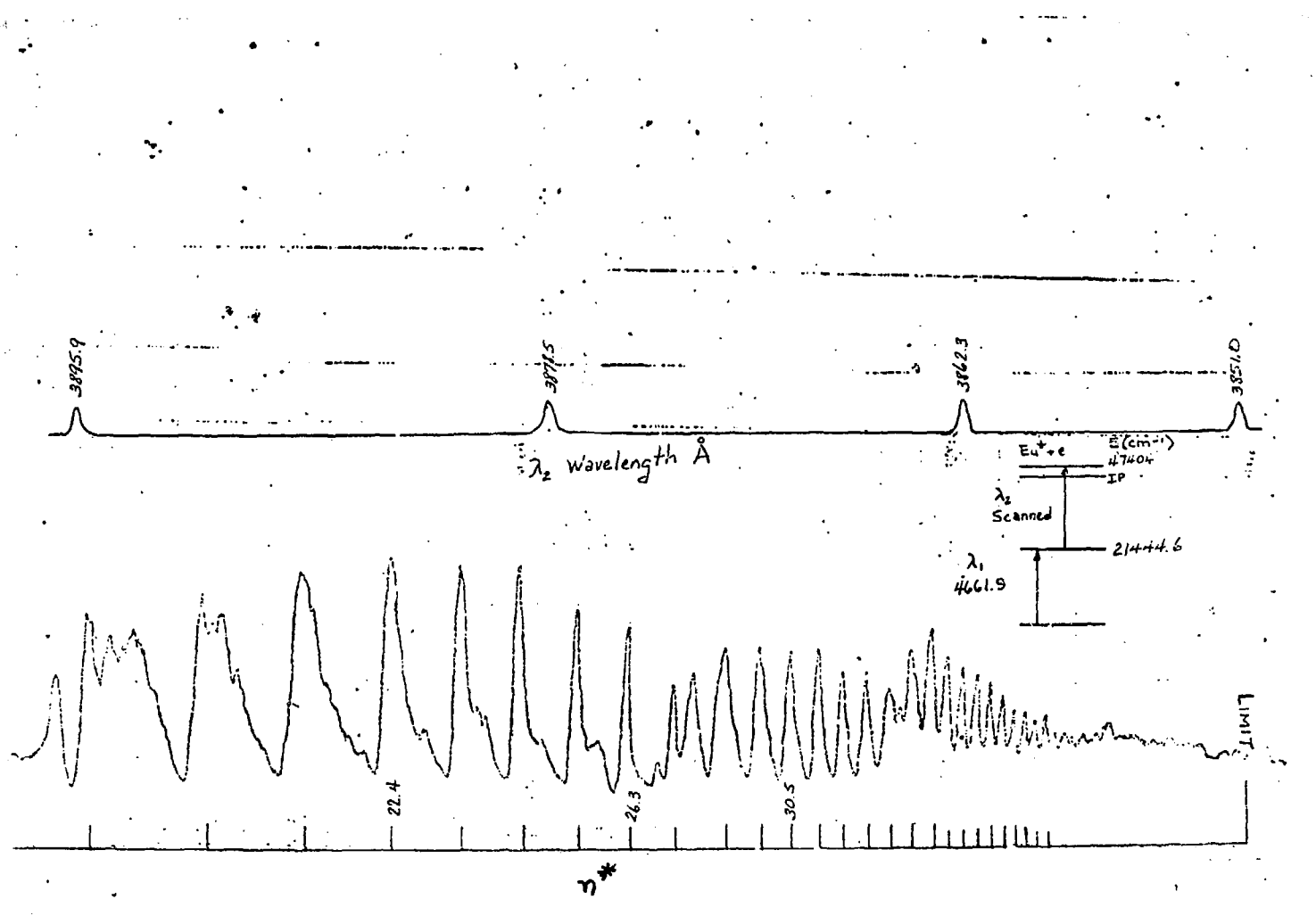

Figure 4. EuI Rydberg Series from the 21444.6 Level Converging to the $^{7}S^{\circ}_{5}$ Limit 1669.2 cm^{-1} above the $^{9}S^{\circ}_{4}$ Ground State of Eu

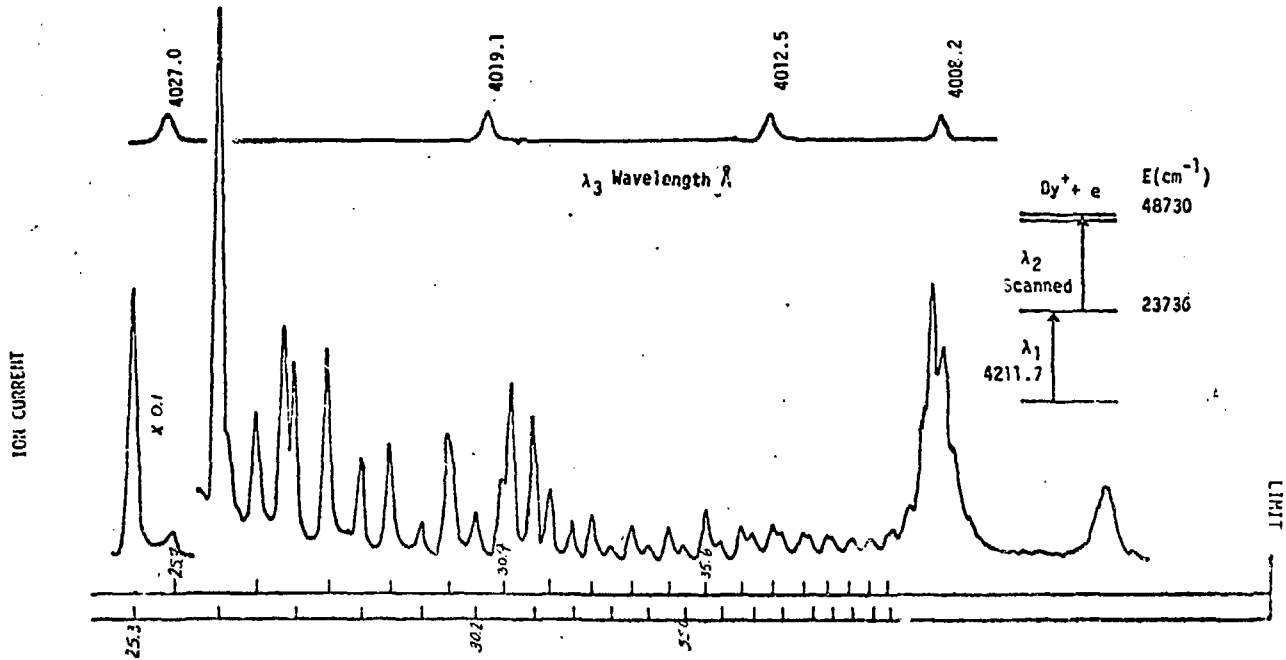

Figure 5. Dysprosium Autoionizing Rydberg Series Converging to the 828 cm^{-1} $^6I_{15/2}$ Level of the Ion.

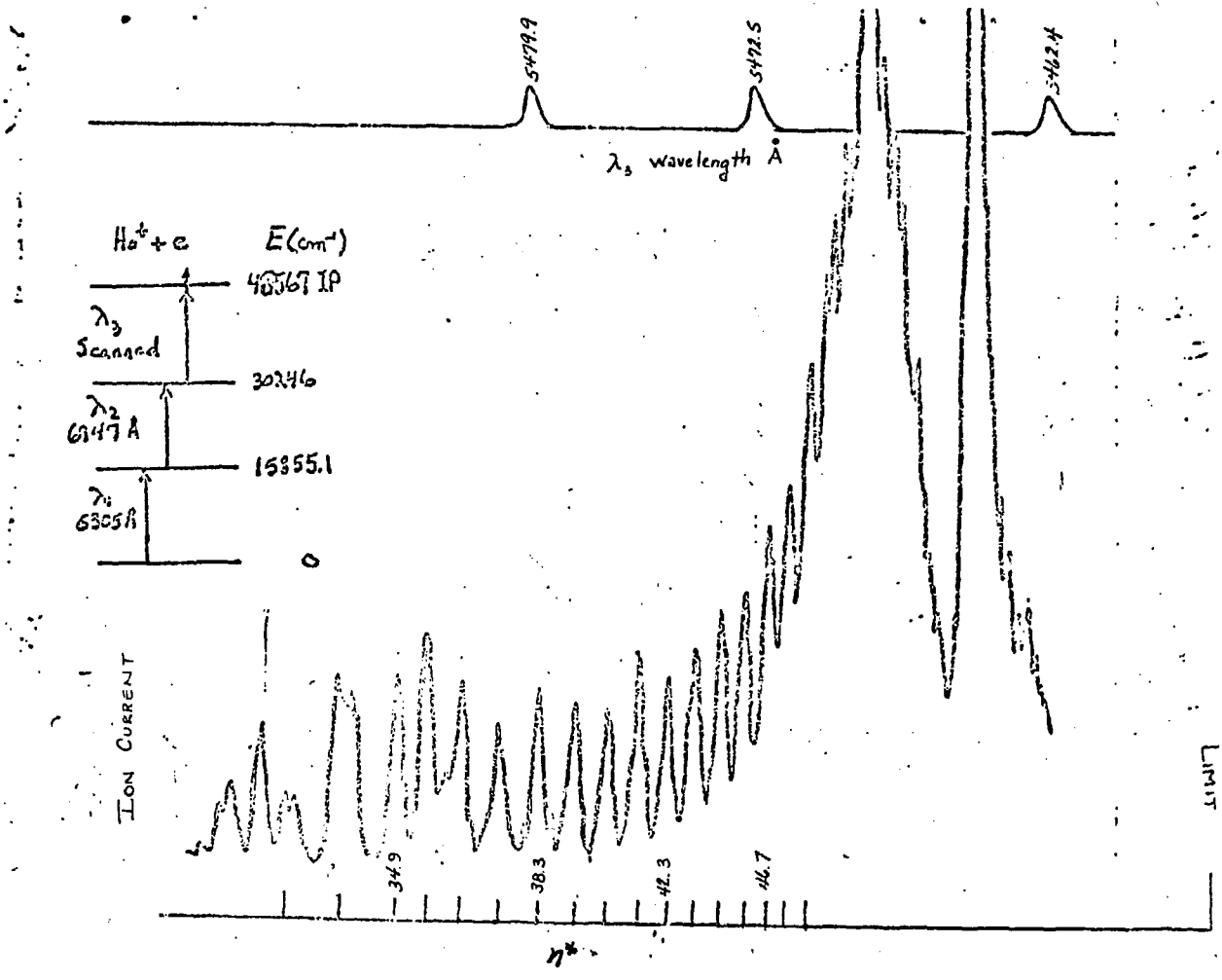

Figure 6. Ho Rydberg Series Converging to the Ground State of the Ion.

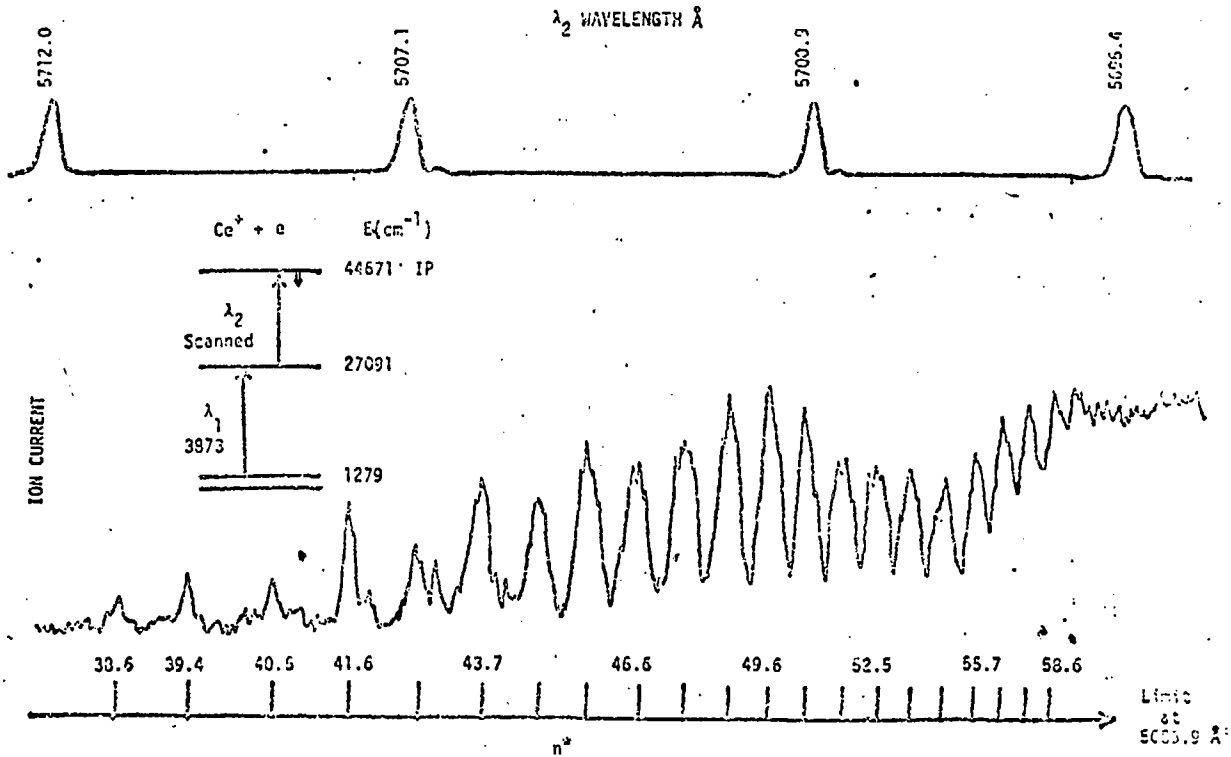

Figure 7. Cerium I Rydberg Series Converging to the Ion Ground State.

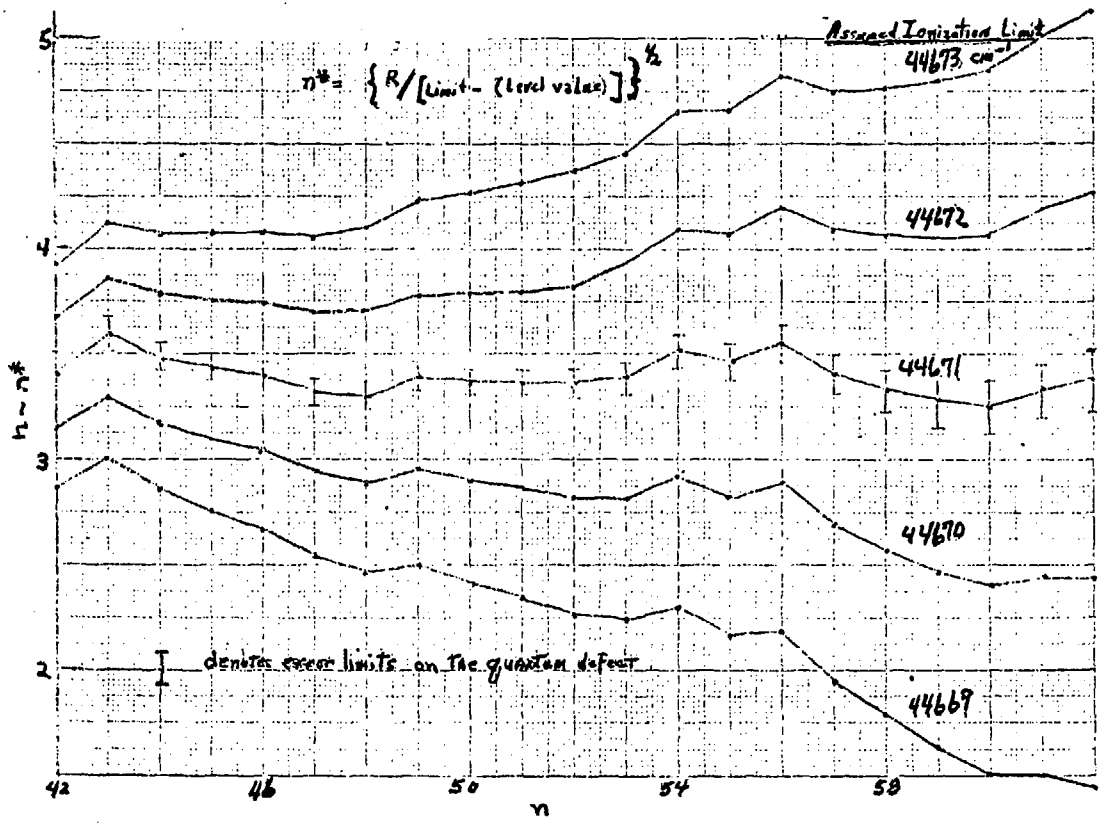

Figure 8. Quantum Defect (n-n*) vs. n for Ce Rydberg Series from the 27091 cm^{-1} Converging to the Ground State of the Ion .

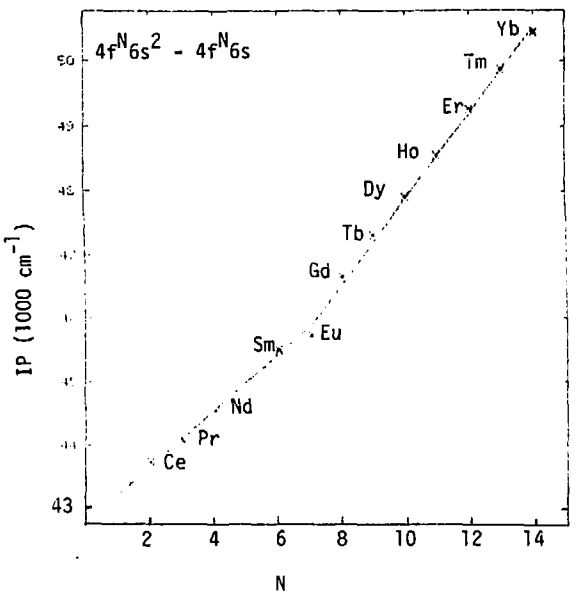

$$IP = \begin{cases} 441\ N + 42822\ cm^{-1} & \text{for } N \leq 7 \\ 661\ N + 41280\ cm^{-1} & \text{for } N \geq 7 \end{cases}$$

Figure 9. Normalized Ionization Potentials of the Lanthanides

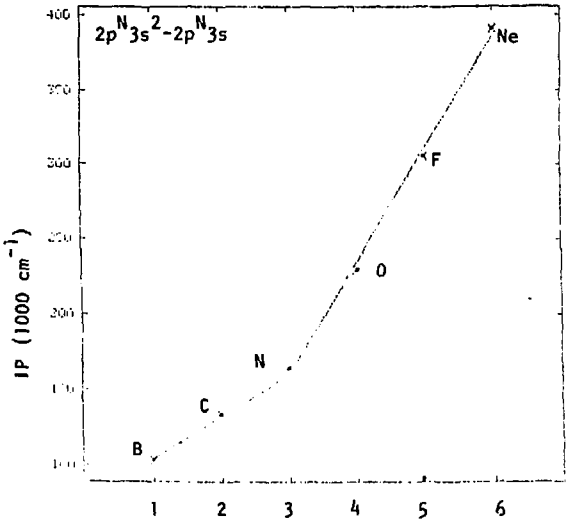

Figure 10. Normalized Ionization Potentials for the 2p Series.

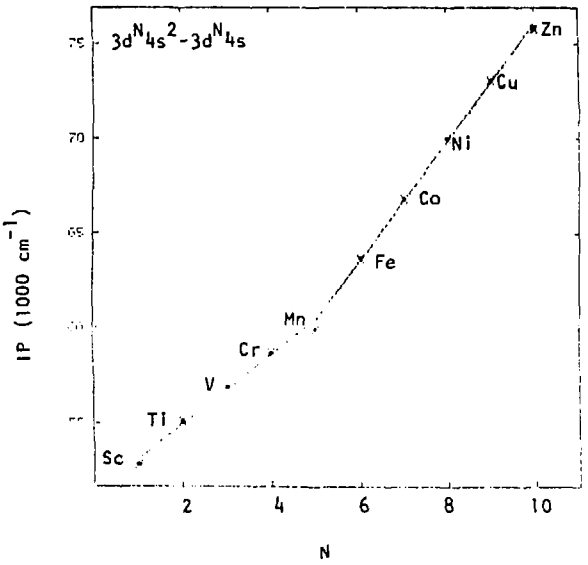

Figure 11. Normalized Ionization Potentials for the 3d or Iron Series.